Journal of
Applied & Computational Mathematics

Elazem et al., J Appl Computat Math 2015, 4:4
DOI: 10.4172/2168-9679.1000235

Research Article Open Access

Radiation Effect of MHD on Cu-water and Ag-water Nanofluids Flow over a Stretching Sheet: Numerical Study

Nader Y Abd Elazem[1]*, Abdelhalim Ebaid[1] and Emad H Aly[2,3]

[1]Department of Mathematics, Faculty of Science, University of Tabuk, Tabuk 71491, Saudi Arabia
[2]Department of Mathematics, Faculty of Science, King Abdulaziz University, Jeddah 21589, Saudi Arabia
[3]Department of Mathematics, Faculty of Education, Ain Shams University, Roxy, Cairo 11757, Egypt

Abstract

Recently, the flow and heat transfer of nanofluids has attracted much attention due to their wide applications in industry and engineering. In this paper, the authors introduce numerical investigation for the effect of radiation on the steady magnetohydrodynamic (MHD) flow and heat transfer of Cu-water and Ag-water nanofluids flow over a stretching sheet. In addtion, the effects of various physical parameters such as, radiation, solid volume fraction, suction/injection and magnetic on involved phenomena are discussed in details through graphs. The numerical results reveal that as parameter of radiation increases, the rate of energy transported to the fluid increases, consequently an increase in temperature occurs. Also, the velocity profile of the Ag–water nanofluid is relatively less than that of the Cu–water nanofluid by increasing the volume fraction and suction/injection parameters while, the converse is valid in the case of the temperature profile. Finally, It is observed that the Ag–water nanofluid has higher skin friction coefficient than the Cu–water nanofluid while, a converse behaviour is found in the case of the Nusselt number.

Keywords: Nanofluids; Stretching sheet; Radiation; MHD; ChCM

Introduction

There are wide-ranging of applications of flow and heat transfer over a stretching surface in many engineering processes, such as polymer extrusion, wire drawing, continuous casting, manufacturing of foods and paper, glass fiber production, stretching of plastic films, and many others. During the manufacture of these sheets, the melt issues from a slit and is subsequently stretched to achieve the desired thickness. The final product with the desired characteristics strictly depends upon the stretching rate, the rate of cooling in the process, and the process of stretching. In addition, due to the numerous applications of nanofluids flow, it has attracted many researchers, examples include nanofluid adhesive: electronics cooling, vehicle cooling, transformer cooling, super powerful and small computers cooling and electronic devices cooling; medical applications: cancer therapy and safer surgery by cooling and process industries; materials and chemicals: detergency, food and drink, oil and gas, paper and printing and textiles. Ultra high-performance cooling is necessary for many industrial technologies [1-3].

Choi [4,5] was the first to introduce the word nanofluid that represent the fluid in which nanoscale particles (diameter<50 nm) are suspended in the base fluid. With the rapid advances in nanotechnology, many inexpensive combinations of liquid/particles are now available. The base fluids used are usually water, ethylene glycol and oil. Recent research on nanofluids showed that nanoparticles changed the fluid characteristics because thermal conductivity of these particles was higher than convectional fluids. Nanoparticles are of great scientific interest as they are effectively a bridge between bulk materials and atomic or molecular structures. Masuda et al. [6], Lee et al. [7], Xuan and Li [8], and Xuan and Roetzel [9] stated that with low nanoparticles concentrations (1–5 Vol%), the thermal conductivity of the suspensions can increase more than 20%. Such an increase depends mainly on several factors such as the form and size of the particles and their concentration, the thermal properties of the base–fluid as well as those of the particles. Hence, the nanofluids can constitute an interesting alternative for advanced applications in heat transfer in the future, especially those in micro scale, see for example [7]. In view of the above applications, Aly and Ebaid [10] studied recently the flow over an isothermal stretching sheet with existence of the most five common nanoparticles, namely, Silver, Copper, Alumina, Titania, and Silicon Dioxide, in a base of water. The main conclusion of this research was that; Silver is the suitable nanoparticle if slowing down the velocity and increasing the temperature are needed; on the other hand, Silicon Dioxide is the appropriate nanoparticle if vice versa behaviour is to be considered.

Magnetohydrodynamics (MHD) boundary-layer flow of nanofluid and heat transfer over a stretching surface have received a lot of attention in the field of several industrial, scientific, and engineering applications in recent years. The comprehensive references on this topic can be found in the some review papers, for example, [11-18] investigated the effects of thermal radiation and magnetic field on the boundary layer flow of a nanofluid over a stretching surface. In addition, Hamad et al. [19] studied the effect of radiation on heat and mass transfer in MHD stagnation point flow over a permeable flat plate with thermal convective surface boundary condition, temperature dependent viscosity and thermal conductivity. Kameswaran et al. [20] studied the combined effects of a magnetic field, viscous dissipation, chemical reaction and Soret effects on nanofluid flow with heat and mass transfer over a stretching or shrinking sheet. They found that the velocity profile decreases with an increase in nano particle volume fraction, while the opposite is true in the case of temperature and

***Corresponding author:** Nader Y. Abd Elazem, Department of Mathematics, Faculty of Science, University of Tabuk, Tabuk 71491, Saudi Arabia, Tel: +96614 42730; E-mail: nelnafrawy@ut.edu.sa

Received June 18, 2015; **Accepted** July 15, 2015; **Published** July 21, 2015

Citation: Elazem NYA, Ebaid A, Aly EH (2015) Radiation Effect of MHD on Cu-water and Ag-water Nanofluids Flow over a Stretching Sheet: Numerical Study. J Appl Computat Math 4: 235. doi:10.4172/2168-9679.1000235

concentration profiles. Very recently, Aly and Sayed [21] investigated effect of the thermal radiation and variable transverse magnetic field on the heat transfer to nanofluids over a steady non-linearly stretching sheet using different types of nanoparticles as Copper, Alumina and Titania Oxide in the base fluid of water. They found that both velocity and temperature profiles increase with increasing the solid volume fraction as well as the velocity distribution decreases whereas the temperature distribution increases with increasing velocity power index and magnetic parameter. However, it decreases with increasing the radiation parameter. Further results of MHD flow of nanofluids over an exponentially stretching sheet were recently presented [22-24].

Motivated by the above studies, the objective of the present study is to extend the research of Kameswaran et al. [20] to study the more general problem which includes the influence of radiation for steady magnetohydrodynamic (MHD) on Cu-water and Ag-water nanofluids flow over a stretching sheet. The dimensionless nonlinear ordinary differential equations will be solved numerically using Chebyshev collocation method as in Section 3 [25].

Mathematical Formulation

In this research, we propose to magnetohydrdynamic (MHD) flow of a nanofluid over a stretching sheet with radiation and effects, in which the flow is incompressible and steady state, where the model that describes this model can be written in dimensional form as [20]**:**

$$\frac{\partial u}{\partial x}+\frac{\partial v}{\partial y}=0, \tag{1}$$

$$u\frac{\partial u}{\partial x}+v\frac{\partial u}{\partial y}=\frac{\mu_{nf}}{\rho_{nf}}\frac{\partial^2 u}{\partial y^2}-\frac{\sigma B_0^2}{\rho_{nf}}u, \tag{2}$$

$$u\frac{\partial T}{\partial x}+v\frac{\partial T}{\partial y}=\alpha_{nf}\frac{\partial^2 T}{\partial y^2}+\frac{\mu_{nf}}{(\rho Cp)_{nf}}\left(\frac{\partial u}{\partial y}\right)^2-\frac{1}{(\rho Cp)_{nf}}\frac{\partial q_r}{\partial y}, \tag{3}$$

with the boundary conditions

$$u=u_w(x)=d(bx),\qquad v=-s,\qquad T=T_w=T_\infty+A\left(\frac{x}{l}\right)^2, at \qquad y=0,$$

$$u\to 0,\quad T\to T_\infty,\qquad at \qquad y\to\infty. \tag{4}$$

where, u and v are the velocity components in the x and y directions respectively, μ_{nf} is the effective dynamic viscosity of the nanofluid, ρ is the fluid density, ρ_{nf} is the effective density of the nanofluid, σ is the electric conductivity, B_0 is the uniform magnetic field strength, α_{nf} is the thermal diffusivity of the nanofluid and $(\rho Cp)_{nf}$ is the heat capacitance of the nanofluid. The velocity of surface is linear and it can be represented as $u=u_w(x)=d(b\,x)$, where d=1 denotes stretching sheet, b is a constant and x is the coordinate measured along the stretching surface. Further, y is the vertical coordinate measuring normal to the surface of sheet. It is assumed that the base fluid is water and the nanoparticles of two different types (Copper and Silver) are in thermal equilibrium and no slip occurs between them. The thermophsical properties of the nanofluid are given in Table 1.

A stream function ψ satisfies the continuity equation (1) such that

$$u=\frac{\partial\psi(x,y)}{\partial y},\ v=-\frac{\partial\psi(x,y)}{\partial x}.$$

	ρ (kg/m³)	C_p (J/Kg K)	k(W/m K)	β×10⁵(K⁻¹)
Pure water	997.1	4179	0.613	21
Copper (Cu)	8933	385	401	1.67
Silver (Ag)	10500	235	429	1.89

Table 1: Thermophysical properties of the water and nanoparticles [25].

By using the following similarity variables:

$$u=bxf'(\eta),v=-(b\nu_f)^{\frac{1}{2}}f(\eta),T=T_\infty+(T_w-T_\infty)\,g(\eta),\eta=\left(\frac{b}{\nu_f}\right)^{\frac{1}{2}}y,\psi=(b\nu_f)^{\frac{1}{2}}xf(\eta), \tag{5}$$

the governing equations of momentum and energy converted into nonlinear ordinary differential equations:

$$f'''(\eta)-C_1\left(f'^2(\eta)-f(\eta)f''(\eta)+\frac{1}{C_2}Mf'(\eta)\right)=0, \tag{6}$$

$$(1+R)g''(\eta)-Pr\frac{k_f}{k_{nf}}C_3\left(2f'(\eta)\,g(\eta)-f(\eta)g'(\eta)-\frac{1}{C_4}Ec\left(f''(\eta)\right)^2\right)=0, \tag{7}$$

with the boundary conditions

$$f(0)=s,\quad f'(0)=d,\quad f'(\infty)=0,\quad g(0)=1,\quad g(\infty)=0, \tag{8}$$

Where (η) and $g(\eta)$ are the dimensionless of the stream function and temperature, respectively. η is the similarity variable, the prime denotes differentiation with respect to η. M, Pr, R, Ec and s denote the magnetic parameter, Prandtl number, radiation parameter, Eckert number and suction parameter (for s > 0) or injection parameter (for s < 0). They are defined as

$$M=\frac{\sigma B_0^2}{b(\rho_f)},\qquad Pr=\frac{\nu_f(\rho Cp)_f}{k_f},\qquad R=\frac{16\sigma^* T_\infty^3}{3k^* k_{nf}},\qquad Ec=\frac{u_w^2}{(Cp)_f(T_w-T_\infty)}.$$

Further, the parameters C_1 to C_4 in Eqs. (6) and (7) are defined as [26]

$$C_1=(1-\varphi)^{2.5}\left(1-\varphi+\varphi\frac{\rho_s}{\rho_f}\right),\quad C_2=1-\varphi+\varphi\frac{\rho_s}{\rho_f},\quad C_3=1-\varphi+\varphi\frac{(\rho Cp)_s}{(\rho Cp)_f},$$

$$C_4=(1-\varphi)^{2.5}\left(1-\varphi+\varphi\frac{(\rho Cp)_s}{(\rho Cp)_f}\right),$$

where φ is the solid volume fraction, ρ_f and ρ_z are the densities of the basic fluid and nanoparticle, $(\rho Cp)_f$ and $(\rho Cp)_s$ are the specific heat parameters of the basic fluid and nanoparticle, and k_s are the thermal conductivities of the basic fluid and nanoparticle, respectively. The thermal conductivity of nanofluids defined [27,28].

$$\frac{k_{nf}}{k_f}=\frac{k_s+2k_f-2\varphi(k_f-k_s)}{k_s+2k_f+\varphi(k_f-k_s)}.$$

By using the Rosseland diffusion approximation [29,30] the radiative heat flux q_r is given by:

$$q_r=-\frac{4\sigma^*}{3k^*}\frac{\partial T^4}{\partial y},$$

Where σ^* is the Stefan-Boltzman constant and k^* is the Rosseland mean absorption coefficient. Assuming that the temperature differences within the flow are sufficiently small such that T^4 may expressed as a linear function of temperature $T^4\cong 4T_\infty^3T-3T_\infty^4$, consequently,

$$\frac{\partial q_r}{\partial y}=-\frac{16\,\sigma^*T_\infty^3}{3k^*}\frac{\partial^2 T}{\partial y^2}.$$

The quantities of practical interest are the skin friction coefficient and the Nusselt number which are defined by

$$C_f(1-\varphi)^{2.5}\sqrt{Re_x}=-2f''(0),\qquad \frac{Nu_x}{\sqrt{Re_x}}\left(\frac{k_f}{k_{nf}}\right)=-(1+\mathrm{R})g'(0). \tag{9}$$

Where Re_x represents the local Reynolds number defined as

$Re_x = \frac{x u_w}{\nu_f}$. When R=s=0, d=1 (for stretching sheet), the system (6-7) is yields to Kameswaran et al. [20]. In the next section, a full description of the Chebyshev collocation method is presented.

Numerical Solution

An efficient Chebyshev collocation method (ChCM) has been employed to study the flow model for the non-linear ordinary differential equations (6-7) with the boundary conditions (8) for different values of governing parameters. The derivatives of the function f(x) at the Gauss-Lobatto points, $x_k = \cos\left(\frac{k\pi}{L}\right)$, which are the linear combination of the values of the function f(x) [31]

$$f^{(n)} = D^{(n)} f,$$

Where,

$$\underset{-}{f} = [f(x_0), f(x_1), \ldots, f(x_L)]^T,$$

and

$$\underset{-}{f^{(n)}} = \left[f^{(n)}(x_0), f^{(n)}(x_1), \ldots, f^{(n)}(x_L)\right]^T$$

Where,

$$D^{(n)} = [d_{k,j}^{(n)}],$$

or

$$f^{(n)}(x_k) = \sum_{j=0}^{L} d_{k,j}^{(n)} f(x_j),$$

where,

$$d_{k,j}^{(n)} = \frac{2\gamma_j^*}{L} \sum_{l=n}^{L} \sum_{\substack{m=0 \\ (m=l-n)\,even}}^{l-n} \gamma_l^* a_{m,l}^n (-1)^{[\frac{lj}{L}]+[\frac{mk}{L}]} x_{lj-L[\frac{lj}{L}]} x_{mk-L[\frac{mk}{L}]},$$

$$a_{m,l}^n = \frac{2^n l}{(n-1)!c_m} \frac{(s-m+n-1)!(s+n-1)!}{s!(s-m)!},$$

such that 2s=l + m - n and c_0=2, c_i=1, i ≥ 1, where k, j=0,1,2,....,L and $\gamma_0^* = \gamma_1^* = \frac{1}{2}, \gamma_j^* = 1$ for j=0,1,2,....,L – 1. The round off errors incurred during computing differentiation matrices $D^{(n)}$ are investigated in [31].

Descriptions of the Method for the Governing Equations

In this section the non-linear ordinary differential equations (6-7) with the boundary conditions (8) are approximated by using Chebyshev collocation method [32,33]. The grid points (x_i, x_j) in this situation are given as $x_j = \cos\left(\frac{j\pi}{L_2}\right)$, for i=1,…, L_1 – 1, and j=1,…, L_2 – 1. The domain in the *x*–direction is [0,x_{max}] where x_{max} is the length of the dimensionless axial coordinate and the domain in the η-direction is [0, η_{max}] where η_{max} corresponds to η_∞. The domain [0,x_{max}] × [0, η_{max}] is mapped into the computational domain [0,x_{max}] × [-1,1]. These equations are third order in (*η*) and second order in g(*η*) which have been transformed into the following Chebyshev collocation equations [32,33]:

$$\left(\frac{2}{\eta_{max}}\right)^3 \left(\sum_{j=0}^{L^*} d_{j,l}^{(3)} f_l\right) - C_1[\left(\frac{2}{\eta_{max}}\right)^2 \left(\sum_{j=0}^{L^*} d_{j,l}^{(1)} f_l\right)^2 - \left(\frac{2}{\eta_{max}}\right)^2 f_j \left(\sum_{j=0}^{L^*} d_{j,l}^{(2)} f_l\right) + \frac{1}{C_2} M \left(\frac{2}{\eta_{max}}\right) \left(\sum_{j=0}^{L^*} d_{j,l}^{(1)} f_l\right)] = 0, \quad (10)$$

$$(1+R)\left(\frac{2}{\eta_{max}}\right)^2 \left(\sum_{j=0}^{L^*} d_{j,l}^{(2)} g_l\right) - Pr\frac{k_f}{k_{nf}} C_3[2\left(\frac{2}{\eta_{max}}\right) g_j \left(\sum_{j=0}^{L^*} d_{j,l}^{(1)} f_l\right) - \left(\frac{2}{\eta_{max}}\right) f_j \left(\sum_{j=0}^{L^*} d_{j,l}^{(1)} g_l\right) - \frac{1}{C_4} Ec \left(\frac{2}{\eta_{max}}\right)^4 \left(\sum_{j=0}^{L^*} d_{j,l}^{(2)} f_l\right)^2] = 0. \quad (11)$$

This system of equations for unknown f_j, g_j where, j=1(1)L^* is solved by Newton-Raphson iteration technique (take L^*=32). It should be noticed that this method can yield greater accuracy for a smooth solution with far fewer nodes and therefore less computational time than the finite-difference and finite element schemes [34].

Results and Discussion

In order to verify the accuracy of the present results, we have initially compared the values of wall temperature gradient -g′(0) for various values of Pr (Table 2). It is clear that the wall temperature gradient -g′(0) increases with Prandtl numbers. The numerical solutions are in a good agreement with previous findings by Grubka and Bobba [35]. Also, comparison of the skin friction $-f''(0)$ for the present results with those previously published works Kameswaran et al. [20], Hamad [36] and Turkyilmazglu [37] is introduced, (Table 3). It is found that there is an excellent comparison of the skin friction $-f''(0)$ for ChCM results for two different types of nanoparticles with Kameswaran et al. [20] for a stretching sheet at M=R=s=0 and Ec=0.1. Physically, increasing values of M enhances the values of the skin friction $-f''(0)$ which is readily known from the fact that the Lorentz drag force opposes the flow. We considered two different types of nanoparticles, namely, copper and silver, with water as the base fluid (i.e. with a constant Prandtl number Pr=6.7850).

Figures 1-3 depict the effects of parameter φ on the velocity profile f ′(η), the temperature profile g(η) and the skin friction coefficient $-2f''(0)$ for stretching sheet at M=1, Ec=10^{-4}, R=5 and s=5. From Figure 1, it is noted that the velocity profile f′(η) decreases as the parameter φ increases. Also, it is observed that the Cu-water nanofluid is relatively less than that of Ag-water nanofluid. Figure 2 shows that increasing the parameter φ of nanoparticles increases the thermal conductivity of the nanofluid. Consequently, the temperature distribution in a Cu-water nanofluid is lower than that of Ag-water nanofluid this is because, the thermal conductivity of copper is less than that of silver. Figure 3 illustrates that increasing the parameter φ of nanoparticles increases the skin friction coefficient $-2f''(0)$ monotonically to a maximum value before decreasing. The results reported that the skin friction coefficient $-2f''(0)$ in the case of a Ag-water nanofluid are higher than that of a Cu-water nanofluid. Further, it is noted that the Ag-water nanofluid

Pr	Grubka and Bobba [35]	Kameswaran et al. [20]	Present ChCM
0.72	1.0885	1.08852	1.088524104594811
1.0	1.3333	1.33333	1.333333333302961
3.0	2.5097	2.50973	2.509725665773766
10.0	4.7969	4.79687	4.796418239172508
100.0	15.7120	15.71163	16.00496464002131

Table 2: Comparison of the values of wall temperature gradient -g′(0) for various Pr.

M	φ	Hamad et al. [36]	Turkyilmazglu [37]	Kameswaran et al. [20]	Present ChCM
			Cu		
0.0	0.05	1.10892	1.1089199	1.108919904	1.10892302325
	0.10	1.17475	1.1747460	1.174746021	1.17474773156
	0.15	1.20886	1.2088623	1.208862320	1.20886357076
	0.2	1.21804	1.2180438	1.218043809	1.21804495932
1.0	0.05	1.45236	1.4523607	1.452360679	1.45236068018
	0.10	1.46576	1.4657632	1.465763175	1.46576317695
	0.15	1.45858	1.4585816	1.458581570	1.45858157267
	0.2	1.43390	1.4338982	1.433898227	1.43389823276
2.0	0.05	1.72887	1.7288724	1.728872387	1.72887238749
	0.10	1.70789	1.7078920	1.707892022	1.70789202165
	0.15	1.67140	1.6713983	1.671398302	1.67139830153
	0.2	1.62126	1.6212642	1.621264175	1.6212641754
			Ag		
0.0	0.05	1.13966	1.1396597	1.139659703	1.13966206018
	0.10	1.22507	1.2250681	1.225068143	1.22506922082
	0.15	1.27215	1.2721529	1.272152949	1.27215364842
	0.2	1.28979	1.2897880	1.289788016	1.28978860960
1.0	0.05	1.47597	1.4759649	1.475964915	1.47596491530
	0.10	1.50640	1.5063948	1.506394844	1.50639484520
	0.15	1.51145	1.5114514	1.511451360	1.51145136214
	0.2	1.49532	1.4953215	1.495321546	1.49532155036
2.0	0.05	1.74875	1.7487483	1.748774830	1.74874830048
	0.10	1.74289	1.7428881	1.742888091	1.74289050170
	0.15	1.71773	1.7177303	1.717730276	1.71773430912
	0.2	1.67583	1.6758341	1.675834100	1.67583409970

Table 3: Values of $-f''(0)$ for various M and **φ** with Ec=s=R=0 and Pr=6.2 for a stretching sheet.

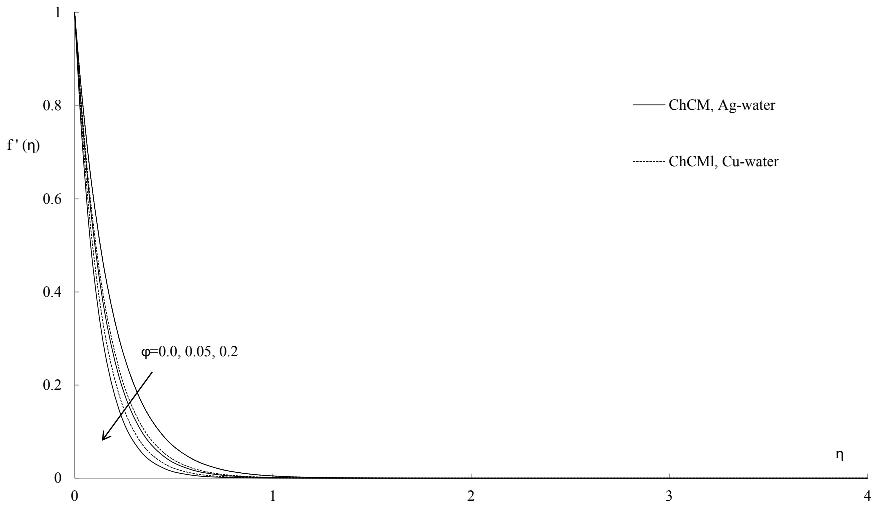

Figure 1: Numerical solution for effects of φ on the velocity profile at d=1, M=1,Ec=10^{-4} , R=5 and s=5.

shows higher drag to the flow as compared to the Cu-water nanofluid.

The effect of radiation parameter R on the temperature g(η) for two different types of nanoparticles, namely, copper and silver, with water as the base fluid of the stretching sheet is depicted in Figure 4. It is seen that as the radiation R increases, the temperature increases. Physically, the amount of $\frac{k^* k_{nf}}{4\,\sigma^* T_\infty^3}$ in the radiation parameter R is the measure of the relative importance of the thermal radiation transfer to the conduction heat transfer. Thus, larger values of this amount show a dominance of the thermal radiation over conduction. Consequently, it indicative of larger amount of radiative heat energy being poured into the system, causing a rise in g(η). As shown in Figure 4 the temperature increases in the Ag-water nanofluid, because the silver, Ag, has higher thermal conductivity (Table 1).

Figures 5-8 illustrate numerical solutions for effects of parameter s on the the velocity profile f '(η), the temperature profile g(η) , the skin fraction coefficient $-2f''(0)$ and the Nusselt number $-(1 + R)\,g'(0)$. It is clear that as parameter s increases, the velocity profile f '(η), and the

Citation: Elazem NYA, Ebaid A, Aly EH (2015) Radiation Effect of MHD on Cu-water and Ag-water Nanofluids Flow over a Stretching Sheet: Numerical Study. J Appl Computat Math 4: 235. doi:10.4172/2168-9679.1000235

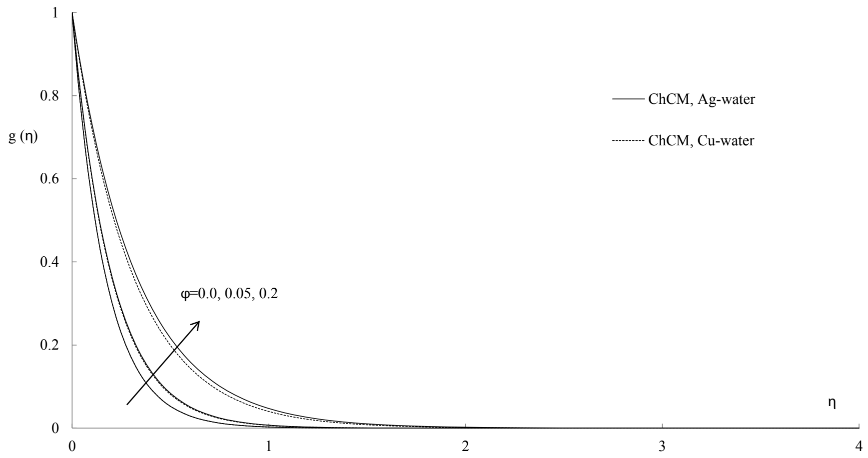

Figure 2: Numerical solution for Effects of φ on the temperature profile at d=1, M=1,Ec=10^{-4}, R=5 and s=5.

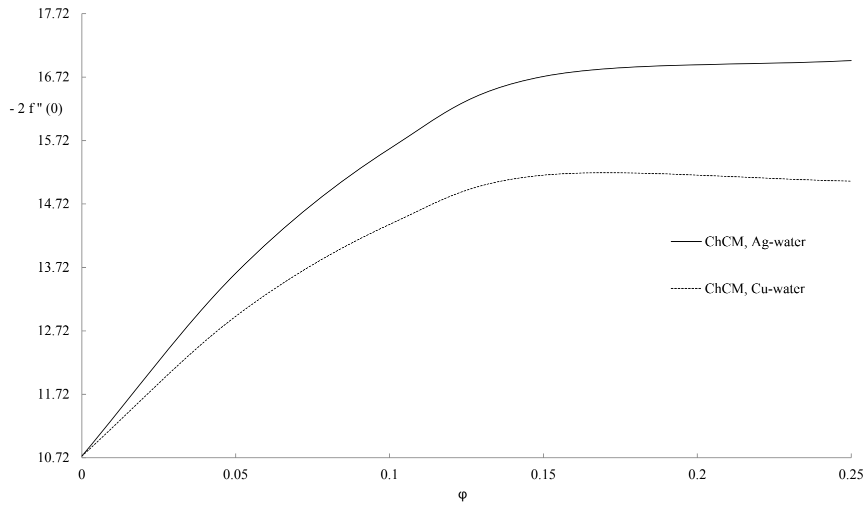

Figure 3: Numerical solution for effects of φ on the skin fraction coefficient at d=1, M=1,Ec=10^{-4}, R=5 and s=5.

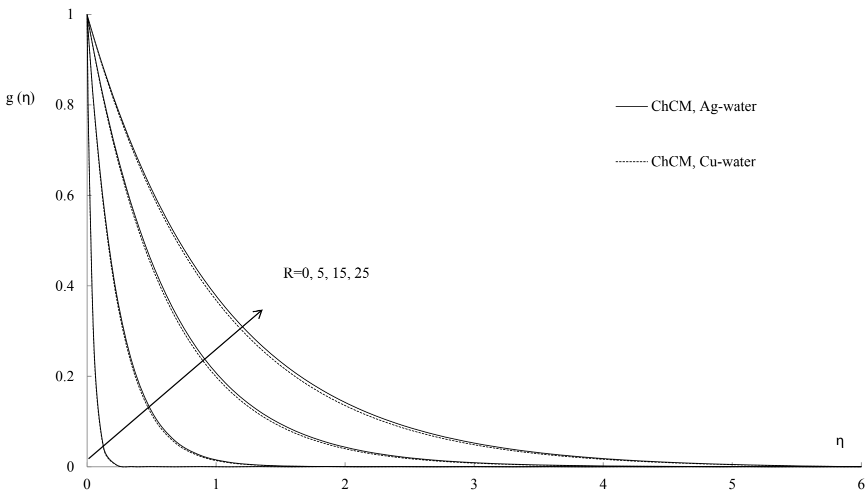

Figure 4: Numerical solution for Effects of R on the temperature profile at d=1, φ=0.1, M=1,Ec=10^{-4} and s=5.

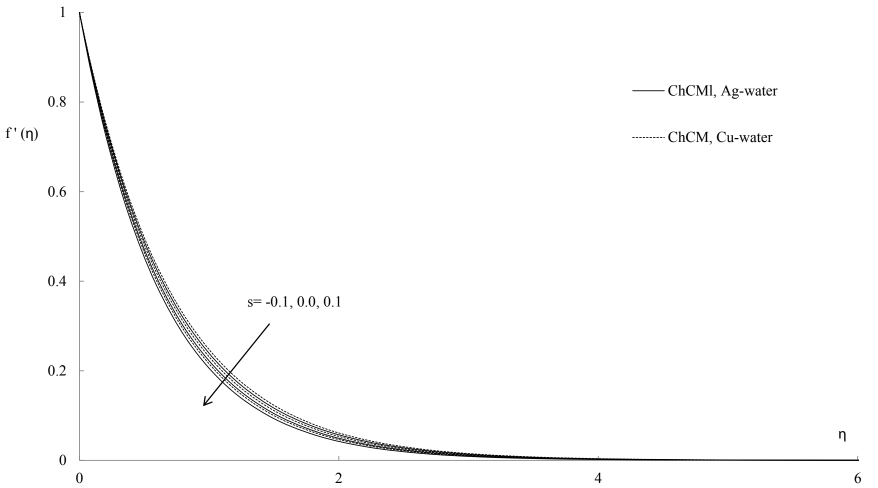

Figure 5: Numerical solution for effects of s on the velocity profile at d=1, φ=0.1, M=1,Ec=10^{-4} and R=5.

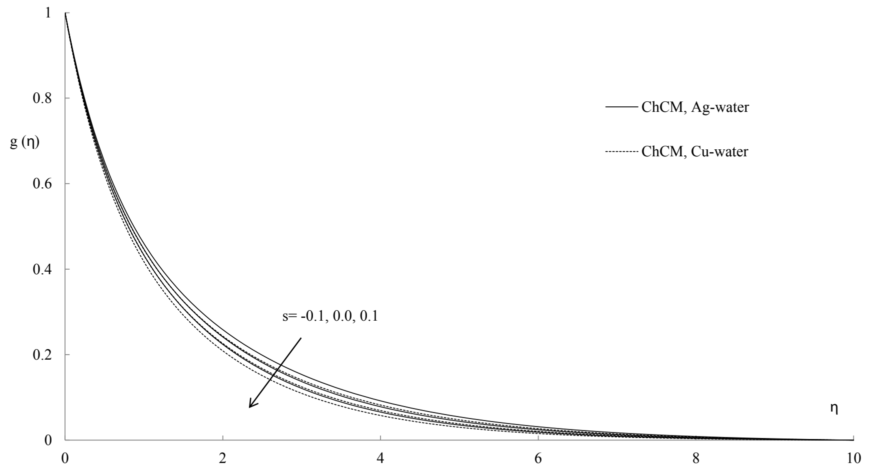

Figure 6: Numerical solution for effects of s on the temperature profile at d=1, φ=0.1, M=1, Ec=10^{-4} and R=5.

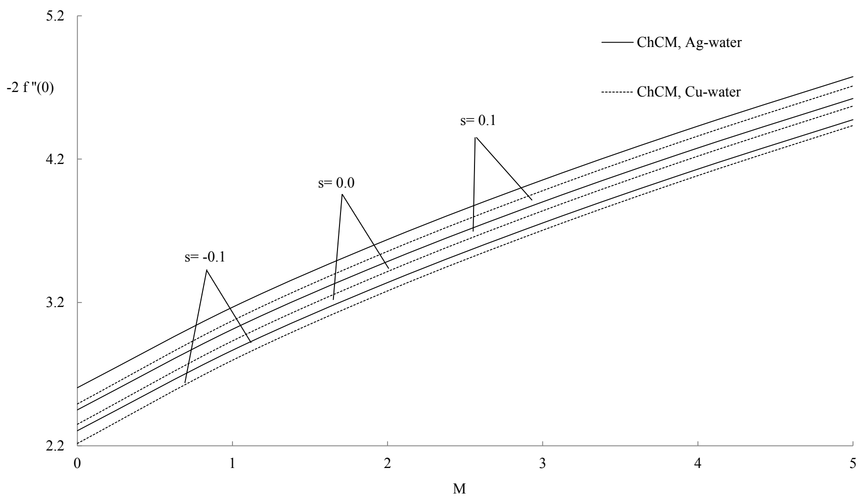

Figure 7: Numerical solution for effects of parameters s and M on the skin fraction coefficient at d=1, φ=0.1,Ec=10^{-4} and R=5.

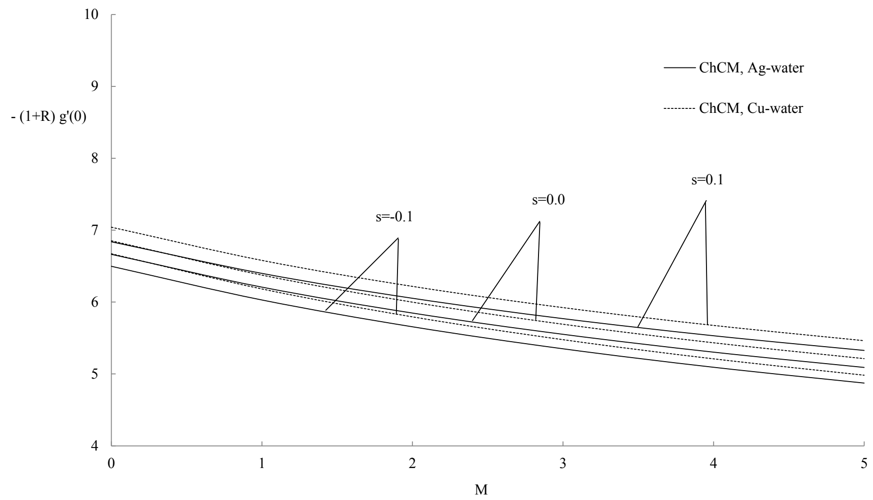

Figure 8: Numerical solution for effects of parametetrs s and M on the Nusselt number at d=1, φ=0.1, Ec=10^{-4} and R=5.

temperature profile g(η) decrease as shown as in Figures 5 and 6. We also observe that velocity profile f '(η), in the case of Ag-water nanofluid is relatively less than that of Cu-water nanofluid while in the oppsite direction the temperature profile g(η) in the case of Ag-water nanofluid is relatively more than that of Cu-water nanofluid. The increase of the parameter s decelerates the fluid motion and decreases the temperature along the sheet. This physical behavior is due to chemical reactions for the combined effects of suction/injection and magnetic parameters. Finally, Figures 7 and 8 depict numerical solutions for effects of parameter s on the skin fraction coefficient $-2f''(0)$ and the Nusselt number $-(1 + R)\, g'(0)$ at d=1, φ=0.1, Ec=10^{-4} and R=5. It should be also noted that Cu-water nanofluid and Ag-water nanofluid behave in different manner. However, the skin fraction coefficient $-2f''(0)$ in the case of a Ag-water nanofluid is bigger than that of a Cu-water nanofluid (Figure 7) but the the Nusselt number $-(1 + R)\, g'(0)$ for the Cu-water nanofluid is bigger than that of the Ag-water nanofluid (Figure 8).

Conclousion

The numerical solution has been performed in this paper for studying a system of ordinary differential equations describing the radiation effect on the boundary layer flow of Cu-water and Ag-water nanofluids. The numerical results, carried out by using the ChCM technique, proved its ability for studying the similar problems with high responsibility. However, the comparison with previous published works is performed and excellent agreement is observed in Tables 2 and 3. For fixed value of radiation parameter and for different two kinds of nanofluids, it has been found that the velocity of the Ag–water nanofluid is relatively less than that of the Cu–water nanofluid by increasing the volume fraction and suction/injection parameters while, the opposite is true in the case of the temperature. It found has been also that as *R* increases, the rate of energy transported to the fluid increases, accordingly an increase in the temperature occurs. In addition, the thermal conductivity of Silver nanoparticle is higher than that of Copper nanoparticle, accordingly, the temperature in the case of a Ag–water nanofluid is relatively higher than that of a Cu–water nanofluid. However, the skin friction coefficient in the case of a Ag–water nanofluid is bigger than that of a Cu–water nanofluid by increasing φ and the combined effects of s and M parameters while, the opposite is valid in the case of the Nusselt number for the combined effects of s and M parameters.

References

1. Altan T, Oh S, Gegel H (1979) Metal Forming Fundamentals and Applications. American Society of Metals, Metals Park, USA.
2. Karwe MV, Jaluria Y (1991) Numerical simulation of thermal transport associated with a continuous moving flat sheet in materials processing, ASME J Heat Transfer 113: 612-619.
3. Kumaran V, Vanav Kumar A, Pop I (2010) Transition of MHD boundary layer flow past a stretching sheet, Commun. Nonlinear Sci Numer Simulat 15: 300-311.
4. Choi SUS (1995) Enhancing thermal conductivity of fluids with nanoparticles, The Proceedings of the 1995 ASME International Mechanical Engineering Congress and Exposition. San Francisco, USA.
5. Choi SUS, Zhang ZG, Yu W, Lockwood FE, Grulke EA (2001) Anomalously thermal conductivity enhancement in nanotube suspensions. Appl Phys Lett 79: 2252-2254.
6. Masuda H, Ebata A, Teramae K, Hishinuma N (1993) Alterlation of thermal conductivity and viscosity of liquid by dispersing ultra-fine particles (Dispersion of g-Al2O3, SiO2, and TiO2 ultra-fine particles). Netsu Bussei 7: 227-233.
7. Lee S, Choi SUS, Li S, Eastman JA (1999) Measuring thermal conductivity of fluids containing oxide nanoparticles. Trans ASME J Heat Transfer 121: 280-289.
8. Xuan Y, Li Q (2000) Heat transfer enhancement of nanofluids. Int J Heat Fluid Flow 21: 58-64.
9. Xuan Y, Roetzel W (2000) Conceptions for heat transfer correlation of nanofluids. Int J Heat Mass Transfer 43: 3701-3707.
10. Aly EH, Ebaid A (2013) Exact analytical solution for suction and injection flow with thermal enhancement of five nanofluids over an isothermal stretching sheet with effect of the slip model: A comparative study. Abstract and Applied Analysis, in the special issue: Mathematical and Computational Analysis of Flow and Transport Phenomena 2013.
11. Chamkha AJ, Aly AM (2011) MHD free convection flow of a nanofluid past a vertical plate in the presence of heat generation or absorption effects. Chem Eng Comm 198: 425-441.
12. Hamad MAA (2011) Analytical solution of natural convection flow of a nanofluid over a linearly stretching sheet in the presence of magnetic field. Int Commu Heat Mass Transfer 38: 487-492.
13. Hamad MAA, Pop I, Md Ismail AI (2011) Magnetic field effects on free convection flow of a nanofluid past a vertical semi-infinite flat plate. Nonlinear Anal Real World Applic 12: 1338-1346.
14. Kandasamy R, Loganathan, Arasu PP (2011) Scaling group transformation for

MHD boundary layer flow of a nanofluid past a vertical stretching surface in the presence of suction/injection. Nuclear Eng Des 241: 2053-2059.

15. Matin MH, Dehsara M, Abbassi A (2012) Mixed convection MHD flow of nanofluid over a non-linear stretching sheet with effects of viscous dissipation and variable magnetic field. Mechanika 18: 415-423.
16. Zeeshan A, Ellahi R, Siddiqui AM, Rahman HU (2012) An investigation of porosity and magnetohydrodynamic flow of non-Newtonian nanofluid in coaxial cylinders. Int J Phys Sci 7: 1353-1361.
17. Khan MS, Mahmud MA, Ferdows M (2011) Finite difference solution of MHD radiative boundary layer flow of a nanofluid past a stretching sheet. In Proceeding of the International Conference of Mechanical Engineering (ICME'11), BUET, Dhaka, Bangladesh.
18. Khan MS, Mahmud MA, Ferdows M (2011) MHD radiative boundary layer flow of a nanofluid past a stretching sheet. In Proceeding of the International Conference of Mechanical Engineering and Renewable Energy (ICMERE '11), CUET, Chittagong, Bangladesh.
19. Hamad MAA, JashimUddin MD, MdIsmail AI (2012) Radiation effects on heat and mass transfer in MHD stagnation-point flow over a permeable flat plate with thermal convective surface boundary condition, temperature dependent viscosity and thermal conductivity. Nuclear Eng Des 242: 194-200.
20. Kameswaran PK, Narayana M, Sibanda P, Murthy PVSN (2012) Hydromagnetic nanofluid flow due to a stretching or shrinking sheet with viscous dissipation and chemical reaction effects. International Journal of Heat and Mass Transfer 55: 7587-7595.
21. Aly EH, Sayed HM (2014) Thermal radiation effects on magnetohydrodynamic boundary-layer flow due to a moving extensible surface in nanofluids. J Comput Theor Nanoscience 11: 1756-1765.
22. Akbar NS, Nadeem S, Ul Haq R, Khan ZH (2013) Radiation effects on MHD stagnation point flow of nano fluid towards a stretching surface with convective boundary condition. Chinese J Aeronautics 26: 1389-1397.
23. Hayat T, Imtiaz M, Alsaedi A, Mansoor R (2014) MHD flow of nanofluids over an exponentially stretching sheet in a porous medium with convective boundary conditions. Chin Phys B 23: 054701
24. Loganathan P, Vimala C (2014) MHD boundary layer flow of a nanofluid over an exponentially stretching sheet in the presence of radiation. Heat Transfer-Asian Research 43: 321-331.
25. Oztop HF, Abu-Nada E (2008) Numerical study of natural convection in partially heated rectangular enclosures filled with nanofluids. Int Heat Fluid Flow 29: 1326-1336.
26. Aminossadati SM, Ghasemi B (2009) Natural convection cooling of a localised heat source at the bottom of a nanofluid-filled enclosure. Eur J Mech B Fluids 28: 630-640.
27. Maxwell JC (1904) Colours in metal glasses and in metallic films, Philos. Trans R Soc Lond A 203: 385-420.
28. Guérin CA1, Mallet P, Sentenac A (2006) Effective-medium theory for finite-size aggregates. See comment in PubMed Commons below J Opt Soc Am A Opt Image Sci Vis 23: 349-358.
29. Hossain MA, Alim MA, Rees DAS (1999) The effect of radiation on free convection from a porous vertical plate. Int J Heat Mass Transfer 42: 181-191.
30. Raptis A (1998) Flow of a micropolar fluid past a continuously moving plate by the presence of radiation. Int J Heat Mass Transfer 41: 2865-2866.
31. Elbarbary EME, El-Sayed MS (2005) Higher order pseudospectral differentiation matrices. Appl Numerical Math 55: 425-438.
32. Abd Elazem NY, Ebaid A (2013) Numerical study of some nonlinear wave equations via Chebyshev collocation method. IJST 37: 477-482.
33. Abd Elazem NY, Ebaid A (2011) Comparison of numerical methods for nano boundary layer flow. Z Naturforsch 66: 539-542.
34. Boyd JP (1989) Chebyshev and Fourier Spectral Methods. Springer-Verlag, New York.
35. Grubka LG, Bobba KM (1985) Heat transfer characteristics of a continuous stretching surface with variable temperature. ASME J Heat Transfer 107: 248-250.
36. Hamad MA, Pop I, Ismali AI (2011) Magnetic field effects on free convection flow of a nanofluid past a vertical semi-infinite flat plate. Non-Linear Anal: Real World Appl 12: 338-346.
37. Turkyilmazoglu M (2012) Exact analytical solution for heat and mass transfer of MHD slip flow in nanofluids. Chem Eng Sci 84: 182-187.